http://rsc.li/frontiers-inorganic

3,5-Bis(4′-carboxylbenzyl)oxy)benzoilate-based coordination polymers: synthesis, structural characterization, and sensing property

Jing-Jing Huang,[a] Xiao Zhang[b],* Qi-Sheng Huo,[a] Jie-Hui Yu,[a],* and Ji-Qing Xu[a]

[a] *College of Chemistry, State Key Laboratory of Inorganic Synthesis and Preparative Chemistry, Jilin University, Changchun, Jilin, 130012, China*

[b] *State Key Lab of Urban Water Resource and Environment (SKLUWRE) & Academy of Fundamental and Interdisciplinary Science, Harbin Institute of Technology, Harbin, Heilongjiang, 150080, China*

Email: jhyu@jlu.edu.cn　　Zhangx@hit.edu.cn

With the assistance of various organic bases, the hydrothermal reactions of transition-metal salts with a kind of tripodal tricarboxylic acid 3,5-bis(4′-carboxylbenzyl)oxy)benzoic acid (H_3(bcbob)) at different pH values were carried out, producing four new bcbob-based 3-D coordination polymers as $[Ni_2(Hbcbob)_2(bimb)_2]$ (bimb = 1,4-bis(imidazol-1-yl-methyl)benzene) **1**, $[Zn_3(bcbob)_2(bpe)_2]$ (bpe = 1,2-bis(4-pyridyl)ethene) **2**, $[H_2(bpp)][Mn_2(bcbob)_2]$ (bpp = 1,2-bis(4-piperidyl)propane) **3**, and $[Cd_2(OH)(bcbob)(bpe)_{0.5}]\cdot H_2O$ **4**. X-ray single-crystal diffraction analysis reveals that (i) in **1**, the bcbob molecules link the Ni^{2+} centers into a 2-D layer with a (6,3) net, then the bimb molecule serves as the pillar linker; (ii) in **2**, the bpe molecule is only used to stabilize the 3-D network. The bcbob molecules link two types of tetrahedral Zn^{2+} ions into a 3-D network with a pcu topology; (iii) the 3-D networks of **3** and **4** are both constructed up from the carboxylate-bridged rod-shaped secondary building units (SBUs) by the bcbob molecules (acting as a 3-connected node), and three types of 1-D channels are observed. However, since the rod-shaped SBUs contain the different structures, the side walls of the channels exhibit the different arrangements. In particular, the side wall in **4** adopts a helical arrangement. The bcbob molecules act as the side wall of the channel. In **3**, the $H_2(bpp)^{2+}$ molecules occupy the space of the largest channels, while in **4**, the bpe molecules occlude one type of smaller channels by coordinating to the Cd^{2+} ions on the side wall. The photoluminescence analysis reveals that **2** and **4** can serve as the chemosensors to detect the ppm-grade nitrobenzene (250 ppm for **2**, 150 ppm for **4**).

Introduction

Considerable attention has been paid to the design and synthesis of novel metal-multicarboxylate coordination polymers (CPs), owing to their structural diversity [1] and the potential applications in some field.[2] For example, (i) due to the stronger ability of forming the clusters or 1-D chains for the metal ions with the carboxylate groups, some metal-multicarboxylate CPs possess the stable 3-D networks with the porous structures, which have been confirmed to be the potential candidates for the H_2 storage and CO_2 capture;[3] (ii) due to the electron deficient nature for nitro-aromatics, it can change the transfer path of the excited electron for the metal-multicarboxylate CPs, leading to the photoluminescence quenching. So the ligand-based photoluminescence metal-multicarboxylate CPs can act as the sensors to detect the trace nitro-explosives;[4] (iii) due to the linkage of the carboxylate groups, the strong M···M interactions may be observed in the metal-multicarboxylate CPs, which makes these materials exhibit the interesting magnetic properties.[5]
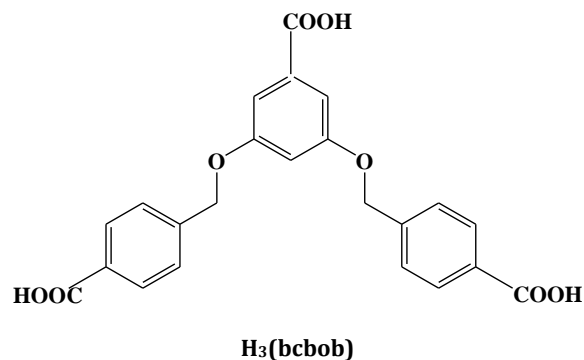
Scheme 1 Molecular structure of $H_3(bcbob)$.

Since a highly porous CP $[Cu_3(tma)_2(H_2O)_3]$ (tma = benzene-1,3,5-tricarboxylate) was reported,[6] some tripodal tricarboxylic acids have been designed, constructing a series of novel metal CP materials over the last fifteen years.[7] However, the semi-rigid 3,5-bis(4′-carboxylbenzyl)oxy)benzoilate (bcbob)-based metal CPs were still less investigated.[8] Scheme 1 plots the molecular structure of the $H_3(bcbob)$ molecule. So called semi-rigidity means that two benzene rings on the 3-, and 5-positions can freely rotate around the $-O-CH_2-$ groups. Due to the existence of two non-metallic atoms, the dihedral angle between two neighboring benzene rings can span a wider range from 0 º to 90 º, compared with those multi-carboxylic molecules without non-metallic atom (dihedral angle: 0 º or a slight rotation) or only with one non-metallic atom (dihedral angle: 90 º or a slight rotation). Furthermore, the $C_6H_5-O-CH_2-H_5C_6$ moiety maybe shows the different shapes: Z or V shape (see Scheme S1). Hence, the framework structure of the as-synthesized bcbob-extended CP is more unpredictable. In addition, the *N,N′*-donor organic bases were mixed into the metal-bcbob reactive system, aiming at (i) extending the metal-bcbob framework, and (ii) stabilizing the metal-bcbob framework structure. In this article, a series of hydrothermal reactions of transition-metal salts and H_3bcbob with the assistance of various *N,N′*-donor organic bases at different pH values were performed, producing finally four new bcbob-based 3-D coordination polymers as $[Ni_2(Hbcbob)_2(bimb)_2]$ (bimb = 1,4-bis(imidazol-1-yl-methyl)benzene) **1**, $[Zn_3(bcbob)_2(bpe)_2]$ (bpe = 1,2-bis(4-pyridyl)ethene) **2**, $[H_2(bpp)][Mn_2(bcbob)_2]$ (bpp = 1,2-bis(4-piperidyl)propane) **3**, and $[Cd_2(OH)(bcbob)(bpe)_{0.5}]·H_2O$ **4**. In order to estimate the properties of the as-synthesized CP materials, the sensing ability of compounds **2** and **4** on the nitrobenzene (NB) molecule was investigated.

Experimental

General

All chemicals are of reagent grade quality, obtained from commercial sources without further purification. Elemental analysis (C, H and N) was performed on a Perkin-Elmer 2400LS II elemental analyzer. Infrared (IR) spectrum was recorded on a Perkin Elmer Spectrum *1* spectrophotometer in 4000-400 cm^{-1} region using a powdered sample on a KBr plate. Powder X-ray diffraction (XRD) data were collected on a Rigaku/max-2550 diffractometer with Cu-K_α radiation (λ = 1.5418 Å). Thermogravimetric (TG) behavior was investigated on a Perkin-Elmer TGA-7 instrument with a heating rate of 10 ºC min^{-1} in air. Fluorescence spectrum was obtained on a LS 55 florescence/phosphorescence spectrophotometer at room temperature.

Syntheses of coordination polymers

[Ni₂(Hbcbob)₂(bimb)₂] 1. A mixture of $Ni(NO_3)_2·6H_2O$ (0.2 mmol, 58 mg), $H_3(bcbob)$ (0.1 mmol, 42 mg),

bimb (0.1 mmol, 24 mg) and water (10 mL) (acidified to pH = 5 by dilute HNO_3), was heated to 150 ^oC in a Teflon-lined stainless steel vessel under autogenous pressure for 4 days, and subsequently cooled to room temperature. The green block crystals of **1** were collected, washed with water, and dried in air. Yield: *ca.* 25% based on Ni(II). Anal. Calcd for $C_{74}H_{60}N_8O_{16}Ni_2$ **1**: C, 61.95; H, 4.21; N, 7.81. Found: C, 61.69; H, 3.97; N, 7.66%. IR (cm^{-1}): 1647 (m), 1593 (m), 1532 (m), 1423 (s), 1294 (w), 1241 (w), 1161 (s), 1109 (w), 1061 (w), 769 (m), 663 (w).

[$Zn_3(bcbob)_2(bpe)_2$] 2. A mixture of $Zn(OAc)_2 \cdot 4H_2O$ (0.2 mmol, 44 mg), $H_3(bcbob)$ (0.1 mmol, 42 mg), bpp (0.1 mmol, 21 mg) and water (10 mL) (neutralized to pH = 7 by dilute NaOH), was heated to 150 ^oC in a Teflon-lined stainless steel vessel under autogenous pressure for 4 days, and subsequently cooled to room temperature. The colorless block crystals of **2** were collected, washed with water, and dried in air. Yield: *ca.* 20% based on Zn(II). Anal. Calcd for $C_{70}H_{54}N_4O_{16}Zn_3$ **2**: C, 59.91; H, 3.88; N, 3.99. Found: C, 59.76; H, 3.68; N, 4.12%. IR (cm^{-1}): 1614 (s), 1568 (s), 1507 (w), 1422 (m), 1343 (m), 1151 (s), 1049 (m), 987 (w), 835 (w), 778 (s), 711 (w), 558 (m).

[$H_2(bpp)$][$Mn_2(bcbob)_2$] 3. A mixture of $MnCl_2 \cdot 4H_2O$ (0.16 mmol, 32 mg), $H_3(bcbob)$ (0.08 mmol, 34 mg), bpp (0.08 mmol, 17 mg) and water (10 mL) (neutralized to pH = 6 by dilute NaOH), was heated to 150 ^oC in a Teflon-lined stainless steel vessel under autogenous pressure for 4 days, and subsequently cooled to room temperature. The colorless block crystals of **3** were collected, washed with water, and dried in air. Yield: *ca.* 20% based on Mn(II). Anal. Calcd for $C_{59}H_{60}N_8O_{16}Ni_2$ **3**: C, 61.95; H, 4.21; N, 7.81. Found: C, 61.69; H, 3.97; N, 7.66%. IR (cm^{-1}): 1591 (s), 1557 (s), 1399 (s), 1373 (s), 1300 (m), 1139 (s), 1041 (m), 854 (w), 821 (w), 775 (m), 756 (w), 708 (w), 629 (w).

[$Cd_2(OH)(bcbob)(bpe)_{0.5}$]·$H_2O$ 4. A mixture of $Cd(OAc)_2 \cdot 2H_2O$ (0.2 mmol, 53 mg), $H_3(bcbob)$ (0.1 mmol, 42 mg), bpe (0.1 mmol, 21 mg) and water (10 mL) (neutralized to pH = 7 by dilute NaOH), was heated to 150 ^oC in a Teflon-lined stainless steel vessel under autogenous pressure for 4 days, and subsequently cooled to room temperature. The colorless block crystals of **4** were collected, washed with water, and dried in air. Yield: *ca.* 18% based on Cd(II). Anal. Calcd for $C_{29}H_{23}NO_{10}Cd_2$ **4**: C, 45.21; H, 3.01; N, 1.82. Found: C, 45.69; H, 3.08; N, 2.16%. IR (cm^{-1}): 1617 (w), 1593 (w), 1507 (w), 1545 (s), 1407 (s), 1367 (s), 1151 (s), 1048 (m), 1020 (w), 855 (w), 825 (w), 767 (m), 550 (m).

X-ray crystallography

The data were collected with Mo-K_α radiation (λ = 0.71073 Å) on a Rigaku R-AXIS RAPID IP diffractometer for **1** and **3**, and on a Siemens SMART CCD diffractometer for **2** and **4**. With SHELXTL program, the structures of all were solved using direct methods.[9] The non-hydrogen atoms were assigned anisotropic displacement parameters in the refinement, and the other hydrogen atoms were treated using a riding model. The hydrogen atoms on C30 in **3**, and on the hydroxyl group in **4** were not located. The hydrogen atom on the carboxyl group in **1** was not located. The lattice water molecule in **4** was confirmed by the elemental analysis and the TG analysis. This method has been extensively employed in the related reports.[10] The structures were then refined on F^2 using SHELXL-97.[9] CCDC numbers are 1059704-1059706 for **1-3**, and 1426333 for **4**, respectively. The crystallographic data for **1-4** are summarized in Table 1.

Table 1 Crystal data of **1-4**.

	1	**2**	**3**	**4**

| Formula	$C_{74}H_{60}N_8O_{16}Ni_2$	$C_{70}H_{50}N_4O_{16}Zn_3$	$C_{59}H_{58}N_2O_{16}Mn_2$	$C_{29}H_{23}NO_{10}Cd_2$
M	1434.72	1399.25	1160.95	770.30
T (K)	293(2)	293(2)	293(2)	293(2)
Crystal system	Triclinic	Monoclinic	Monoclinic	Monoclinic
Space group	P-1	$C2/c$	$C2/c$	$C2/c$
a (Å)	9.1609(18)	45.925(2)	15.338(3)	31.512(3)
b (Å)	12.811(3)	6.5022(3)	22.100(4)	7.0593(4)
c (Å)	14.754(3)	21.3486(15)	16.425(3)	27.1251(19)
α (º)	87.65(3)	90	90	90
β (º)	85.10(3)	105.346(6)	102.64(3)	106.230(4)
γ (º)	89.56(3)	90	90	90
V (Å³)	1723.7(6)	6147.2(6)	5432.6(19)	5793.6(8)
Z	1	4	4	8
D_c (g cm⁻³)	1.382	1.512	1.419	1.766
μ (mm⁻¹)	0.621	1.237	0.539	1.526
Reflections collected	16778	16552	22151	15895
Unique reflections	7711	5397	6199	5106
R_{int}	0.0242	0.0416	0.0512	0.0360
Gof	1.102	1.052	1.050	1.179
R_1, $I>2\sigma(I)$	0.0409	0.0493	0.0560	0.0407
wR_2, all data	0.1176	0.1689	0.1674	0.1331

Results and discussion

Synthetic analysis

All of the reactions are carried out under the hydrothermal conditions. The reactions of transition-metal salts, H_3(bcbob) and organic bases in a molar ration of 2:1:1 at different pH levels were performed, creating the title compounds **1**-**4**. During the reactions, the pH value of the reactive mixture plays a key role. On the one hand, it determines the degree of the deprotonation reaction for H_3(bcbob). At pH ≥ 6, the H_3(bcbob) molecule can be completely deprotonated, and exists in the form of bcbob³⁻, based on the reactions of compounds **2**, **3** and **4**. While at pH = 5, the H_3(bcbob) molecule is partly protonated, and exists in the form H(bcbob)²⁻, based on the reaction of compound **1**. On the other hand, it controls the existing form of the organic base molecule. As observed in compound **3**, bpp exists in a diprotonated form at pH = 6, whereas as observed in compounds **3** and **4**, bpe exists in a neutral molecule at pH = 7. But the bimb molecule is difficult to be protonated at a weakly acidic environment as pH = 5, as found when preparing compound **1**.

Structural description of 1

Compound **1** is a 3-D Ni²⁺ coordination polymer with a mixed ligand of bcbob and bimb. The asymmetric unit of compound **1** is found to be composed of one Ni²⁺ ion (Ni1), one bcbob molecule and one bimb molecule. The organic acidic molecule should exist in the form of H(bcbob)²⁻, in order to balance the systematic charge. The 1-position carboxyl group should be deprotonated, which is revealed by two equivalent C-O distances. While for the other two carboxylate groups, two C-O distances for each are different, suggesting that this H⁺ ion is related to these two carboxylate groups. The bcbob molecule exhibits a triple-bridged coordination mode. As shown in Scheme 2, the 1-position carboxylate group and the carboxylate group on the 3-position benzyloxy group monodentately bond respectively to one Ni²⁺ center, while the carboxylate group on the

5-position benzyloxyl group chelates to one Ni^{2+} center. As shown in Fig. 1b, the $\eta^1:\eta^0:\eta^1:\eta^0:\eta^1:\eta^1:\mu_3$-mode H(bcbob)$^{2-}$ molecules link the Ni^{2+} centers into a 2-D layer network. Based on the topological viewpoint, both the Ni^{2+} center and the bcbob molecule can be regarded as a 3-connected node, so this 2-D layer network possesses a simple (6,3) topology. The bimb molecule serves as the pillar linker, extending the 2-D Ni(Hbcbob) layers into a 3-D network, as shown in Fig. 1a. Synchronously, the 1-D channels form in the 3-D network of compound **1**. However, the 3-fold interpenetration is observed in the packing structure of compound **1**, occluding these channels. The Ni1 center in compound **1** is involved in an octahedral site with four carboxylate O atoms (O2, O4b, O5a, O6a; Ni1-O = 2.0621(16)-2.1466(16) Å) occupying the equatorial plane, and two bimb N atoms (N1, N3; Ni1-N = 2.061(2)-2.062(2) Å) occupying the axial positions (see Fig. S1).

(a) **(b)**
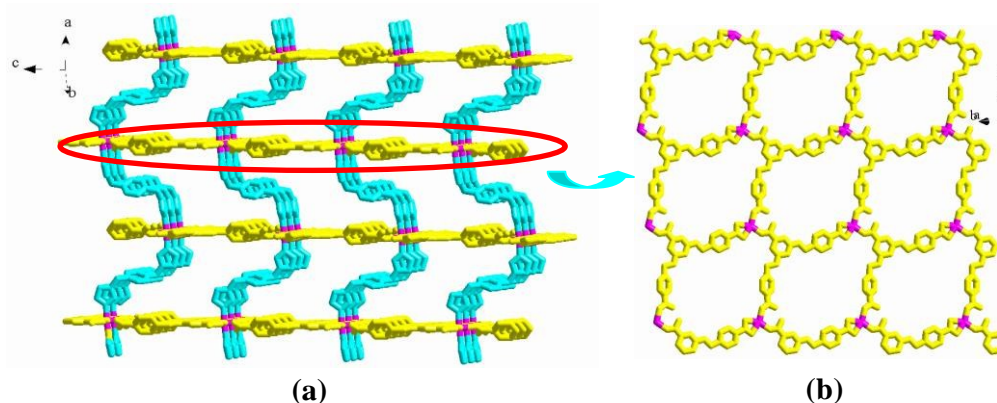
**Fig. 1** 3-D network (a) and 2-D Ni-H(bcbob)$^{2-}$ layer (b) in **1**.

Structural description of 2

Compound **2** is a 3-D Zn^{2+} coordination polymer with a mixed ligand of bcbob and bpe. The asymmetric unit of compound **2** is found to be composed of two types of Zn^{2+} ions (Zn1, Zn2; occupancy ratio: 1 for Zn1, 0.5 for Zn2), one bcbob molecule and one bpe molecule. Zn1 and Zn2 are both involved in a tetrahedral site, but the detailed coordination environments are different (see Fig. S2). Zn1 is coordinate with three carboxylate O atoms (O2a, O3b, O4) and one bpe N atom (N1), whereas Zn2 is completed by two carboxylate O atoms (O6d, O6e) and two bpe N atoms (N2, N2f). As shown in Scheme 2, the bcbob molecule adopts a tetra-bridged coordination mode. Two carboxylate groups interact respectively with one Zn^{2+} ions, whereas the third carboxylate group bridge bidentately to two Zn^{2+} ions. In compound **2**, the bpe molecule plays two roles. One is to complete the tetrahedral coordination of two Zn^{2+} centers, and the other is to stabilize the 3-D network of compound **2**. The bcbob molecules link two types of Zn^{2+} ions to form a 3-D network of compound **2**, as shown in Fig. 2a. The bcbob molecules first utilize two carboxylate groups to serve as the donors, linking the Zn1 ions into a 2-D layer network (see Fig. 2b). This 2-D layer is based on a kind of carboxylate-bridged dimer (see Fig. 2c), which is composed of two Zn1 centers and two carboxylate groups on the 5-position benzyloxy groups. Via the interactions between the Zn1 ion and the 1-position carboxylate O atom (O2a), each dimer interacts with adjacent four dimers, forming finally this 2-D layer network. The other carboxylbenzyloxy groups protrude from the layer. Via the interactions between Zn2 and O6d/O6e, the Zn2 ions act as the bridges, propagating the 2-D layer into a 3-D network of compound **2**. The bpe molecule acts as the second connector to link further Zn1 and Zn2 together, stabilizing the 3-D network of compound **2** (see Fig. 2d). The Zn-O and Zn-N ranges are 1.945(4)-1.966(3) Å and 2.024(4)-2.059(4) Å, respectively.
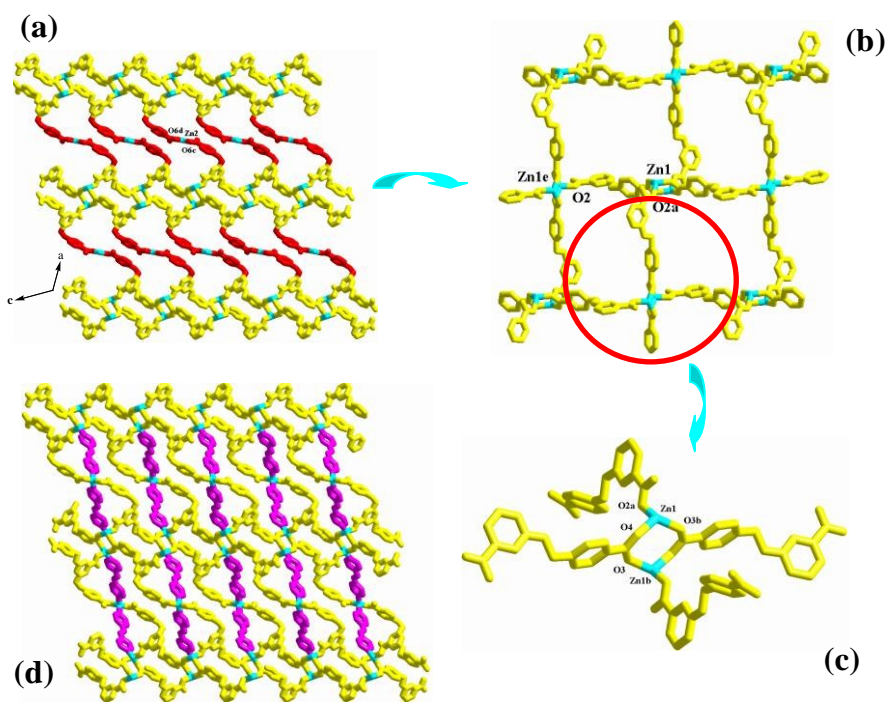
Fig. 2 3-D Zn-bcbob network (a), 2-D (4,4) net (b), dimer (c) and 3-D Zn-bcbob-bpe network (d) in **2** (a: *x*, -*y*+4, *z*+1/2; b: -*x*+1/2, -*y*+5/2, -*z*+2; c: *x*, -*y*+2, *z*+1/2; d: -*x*, -*y*+2, -*z*+1; e: *x*, -*y*+4, z-1/2).

Structural description of 3
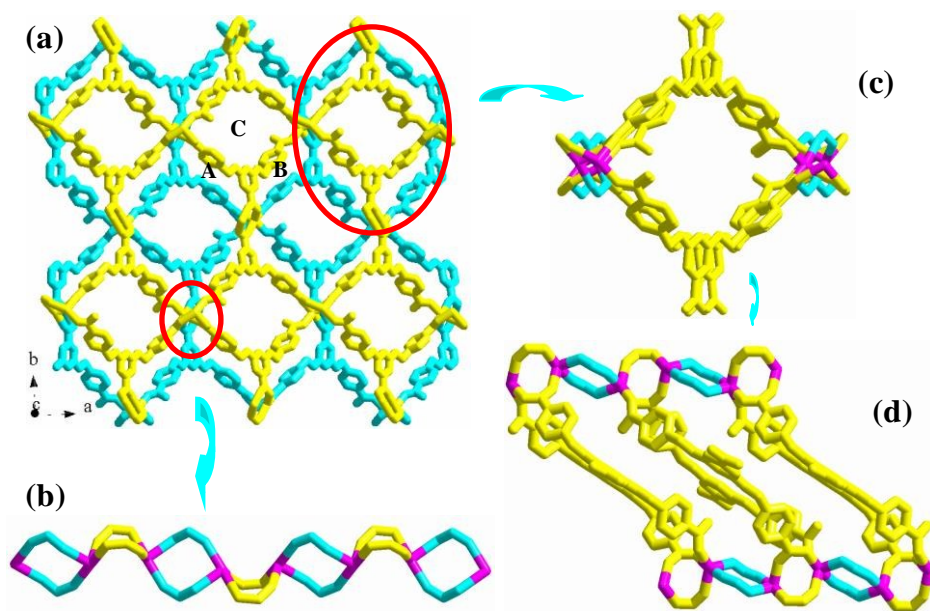
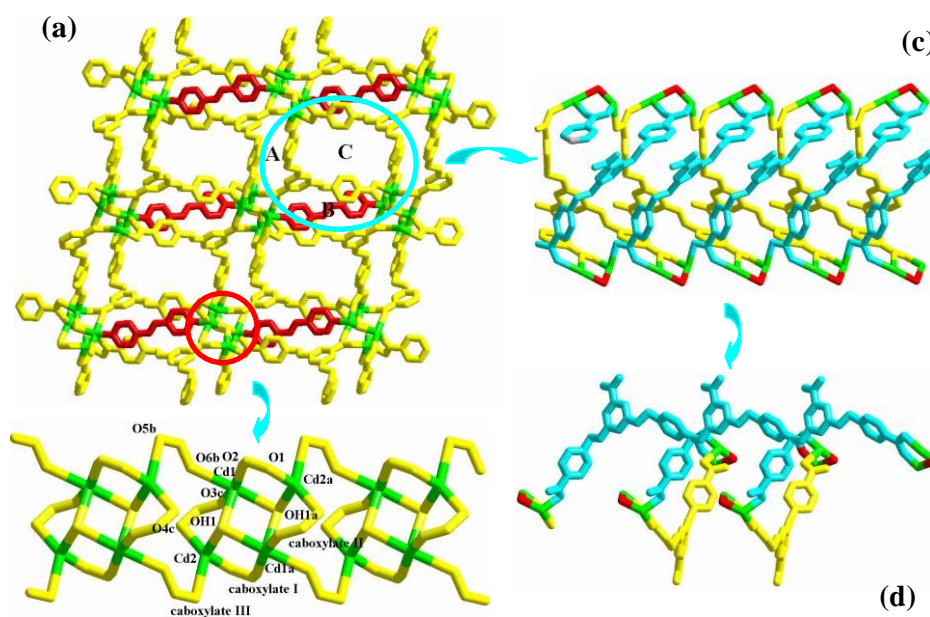**Fig. 3** 3-D network (a), rod-shaped SBU (b), and 1-D channel (c, d) in **3**.

Compound **3** is a bcbob-extended 3-D Mn^{2+} coordination polymer with the occluded $H_2(bpp)^{2+}$ cations. The asymmetric unit of compound **3** is found to be composed of one Mn^{2+} ion (Mn1), one bcbob molecule and a half $H_2(bpp)^{2+}$ molecule. As shown in Fig. S3, Mn1 with a trigonal bipyramidal geometry is coordinate with

five carboxylate O atoms (O1, O3d, O4a, O5b, O6c; Mn1-O = 2.084(2)-2.143(2) Å). The bcbob molecule is involved in a penta-bridged coordination mode: five O atoms monodentately bond to one Mn^{2+} center, respectively (see Scheme 2). Templated by $H_2(bpp)^{2+}$, the penta-bridged bcbob molecules link the 5-coordinated Mn^{2+} centers into a 3-D network structure, as shown in Fig. 3a. The 3-D network is based on the rod-shaped secondary building unit (SBU), which can be described as an alternate arrangement of two types of carboxylate-bridged 8-membered dimers (dimer I, dimer II; see Fig. 3b). The carboxylate groups on 5-position benzyloxy groups doubly bridge two Mn^{2+} ions to construct dimer I, whereas the 1-position carboxylate groups doubly bridge two Mn^{2+} ions to construct dimer II. Two types of dimers show the different arrangements: boat configuration for dimer I, and chair configuration for dimer II. The Mn···Mn separations are 4.973 Å and 3.702 Å, respectively. The bcbob molecule serves as a 3-connected node, extending the rod-shaped SBUs into a 3-D network of compound **3**, where the 1-D channels with the larger rhomboid window are observed (see Fig. 3c). As shown in Fig. 3d, the bcbob molecules with the carboxylate groups on 3,5-position benzyloxy groups doubly bridge two rod-shaped SBUs to form this 1-D channel with the window size of 10 × 9 Å². The bcbob molecules act as the side wall of the channel. The arrangements of two side walls are the same (see Fig. 3d).

Structural description of 4

Fig. 4 3-D network (a), rod-shaped SBU (b), 1-D channel (c) and helical chain (d) in **4** (a: -*x*-1/2, -*y*+1/2, -*z*-1; b: -*x*, *y*-1, -*z*-1/2; c: *x*, -*y*+2, *z*-1/2).

Compound **4** is a 3-D Cd^{2+} coordination polymer with a mixed ligand of bcbob and bpe. The asymmetric unit of compound **4** is found to be composed of two types of Cd^{2+} ions (Cd1, Cd2), one bcbob molecule, a half bpe molecule, and one OH^- group. The triple-bridged O atom is defined as the OH^- group, in order to balance the systematic charge. Two types of Cd^{2+} ions show the different geometries: Cd1 is in an octahedral site, surrounded by three carboxylate O atoms (O2, O3c, O6b), one bpe N atom (N1), and two OH^- groups (OH1, OH1a), whereas Cd2 is in a tetrahedral site, completed by three carboxylate O atoms (O1, O4d, O5e) and one OH^- group (OH1) (see Fig. S4). The bcbob molecule adopts a hexa-bridged coordination mode: each

carboxylate group bidentately bridge two Cd^{2+} centers (See Scheme 2). The OH^- group adopts a trigonal pyramidal geometry with the Cd-OH1-Cd angles of 101.19(14)-107.25(14) ^{o} and a distance of 0.95 Å from the apical OH^- group to the plane being comprised of three Cd(II) ions. As shown in Fig. 4a, compound **4** seems to have a similar 3-D network to that of compound **3**, namely the bcbob molecules as a 3-connected node link the rod-shaped SBUs into a 3-D network with three types of 1-D channels (channel A, channel B, channel C). They are indeed different. In compound **4**, the rod-shaped SBU $Cd_2(OH)(COO)_6$ is based on a kind of tetranuclear cluster. As shown in Fig. 4b, two OH^- groups link two Cd1 ions and two Cd2 ions to form this tetranuclear cluster. The centric Cd_2O_2 ring is planar, and the Cd1···Cd1a separation is 3.605 Å. Each two neighboring Cd^{2+} ions are further bridged by carboxylate I and carboxylate II for the bcbob molecule, stabilizing this cluster structure. Then the carboxylate III groups doubly bridge the adjacent tetranuclear clusters into a chained SBU of compound **4**, extending along the *b*-axial direction. Since the SBU shows the difference, the bcbob molecule also adopts the different arrangement in both compounds (see Fig. 4c). The arrangements on two side walls in compound **4** are different, and a helical chain is found, as shown in Fig. 4d. As shown in Fig. S5, the 3-D network of compound **3** can also be described as an alternate arrangement of two types of layers via sharing the Mn^{2+} centers. A translation of the layer I produces the layer II. However, due to the existence of the helical chain in compound **4**, it is difficult to find out a 2-D layer in the 3-D network of compound **4**. In compound **3**, the $H_2(bpp)^{2+}$ molecules occupy the space of the largest channel C. Channel A has the same window as that of channel B. Whereas in compound **4**, the bpe molecules occlude the space of channel B by coordinating to the Cd^{2+} centers on the side walls. Although the window of channel C turns small, channel C can be activated, and the lattice water molecule occupies its space. The Cd-O range is 2.166(8)-2.414(7) Å, and the Cd-N separation is Cd1···Cd2 = 3.3245(10) Å.

Structural discussion

$\eta^1{:}\eta^0{:}\eta^1{:}\eta^0{:}\eta^1{:}\eta^1{:}\mu_3$ in **1** $\eta^1{:}\eta^0{:}\eta^1{:}\eta^1{:}\eta^1{:}\eta^0{:}\mu_4$ in **2**

$\eta^1{:}\eta^1{:}\eta^1{:}\eta^0{:}\eta^1{:}\eta^1{:}\mu_5$ in **3** $\eta^1{:}\eta^1{:}\eta^1{:}\eta^1{:}\eta^1{:}\eta^1{:}\mu_6$ in **4**
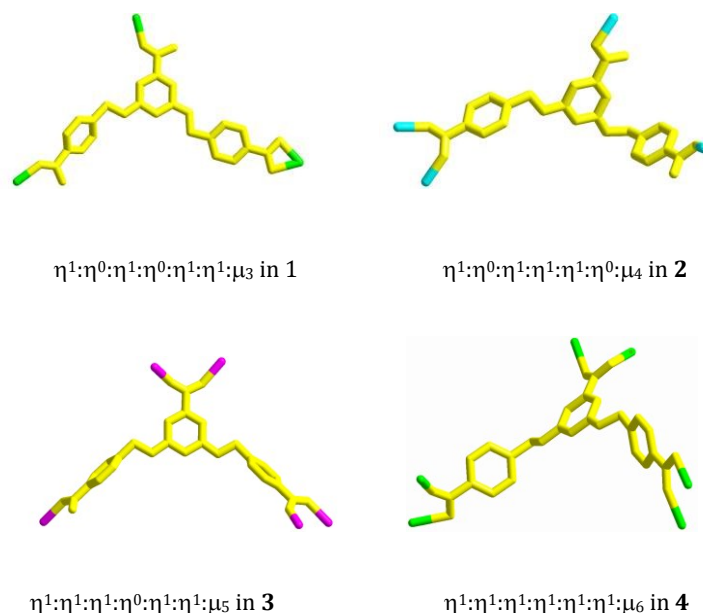
Scheme 2 Coordination modes of bcbob in **1**-**4**.

The title four compounds are all new, different from the reported bcbob-based CPs.[8] All possess the 3-D network structures. The bcbob molecule shows its special semi-rigidity: (i) in compounds **1**-**4**, the dihedral angles of two neighboring benzene rings span a rather wider range from 13.5 ^{o} observed in compound **1**, to

87.7 $^{\circ}$ observed in compound **2**. Note that in compound **1**, two adjacent benzene rings array in a nearly parallel form; (ii) the C_6H_5-O-CH_2-H_5C_6 moiety for bcbob exhibits two shapes. Generally, it adopts a Z-shape arrangement, namely two neighboring benzene rings are distributed on both sides of the CH_2-O line. In compound **2**, the V-shape C_6H_5-O-CH_2-H_5C_6 moiety is observed. As found in compounds **3** and **4**, the porous size of the 3-D M^{2+}-bcbob network can be adjusted by the mixed organic base molecule, which should also be related to the diverse configuration of the C_6H_5-O-CH_2-H_5C_6 moiety. The bcbob molecules can link the metal ions into a 3-D network with the channels. The channel has a larger window. Such a 3-D network is unstable. The main role of the introduced organic base molecule is to stabilize this unstable 3-D network: (i) stabilizing the 3-D network through a way of decreasing the window's size of the channel, namely acting as a so-called pillar to further support the channel, as observed in compounds **2** and **4**; (ii) stabilizing the 3-D network through a way of acting as the guest molecule, as observed in compound **3**. Once the bcbob molecules only link the metal ions into an oligomer, the introduced organic base molecule can serve as the pillar linker, extending the metal-bcbob oligomers into a 3-D network, as observed in compound **1**. Due to the existence of the channel with the larger window, this 3-D network is unstable, either. So a 3-fold interpenetration occurs in compound **1**, in order to form a stable network. Obviously, the most important role of the incorporated organic base molecule is to direct influence the interaction between the metal ion and the bcbob molecule.

Characterization

Fig. S6 presents the experimental and simulated powder XRD patterns of **1-4.** The experimental powder XRD pattern for each compound is in accord with the simulated one generated on the basis of structural data, confirming that the as-synthesized product is pure phase.

The TG behaviors of compounds **1-4** were investigated. Fig. S7 gives the temperature *vs.* weight-loss curves. For the TG curve of compound **4**, a minor weight loss of *ca.* 2.2% is observed in the temperature range of 30-300 $^{\circ}$C, corresponding to the removal of one water molecule (Calcd: 2.3%). This means that in an asymmetric unit of compound **4**, there is one lattice water molecule (see Fig. S8 for better understanding). The C, H and N analysis also supports this conclusion. For the TG curves of compounds **1-3**, no any weight loss is found before 300 $^{\circ}$C, indicating that there are no neutral guest molecules in compounds **1-3**. Based on the TG curves of **1-4**, we also know that (i) compounds **1-4** possess the better thermal stability, because the temperature for the onset of the collapse of the host frameworks are higher: 350 $^{\circ}$C for **1**, 400 $^{\circ}$C for **2**, 350 $^{\circ}$C for **3**, 370 $^{\circ}$C for **4**; (ii) the final residues for all are proved to be the metal (di)oxides: NiO for **1** (Calcd: 10.4%; Found: *ca.* 10.1%), ZnO for **2** (Calcd: 17.4%; Found: *ca.* 18.6%), MnO_2 for **3** (Calcd: 14.9%; Found: *ca.* 13.9%), and CdO for **4** (Calcd: 33.3%; Found: *ca.* 33.2%), respectively. Fig. S9 plots the IR spectra of compounds **1-4**.

Sensing property

(a)   (b)
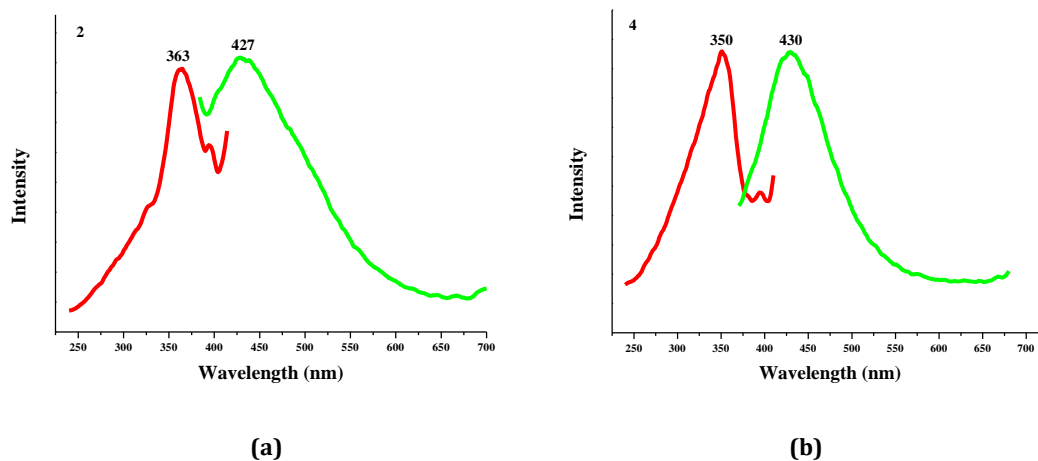
Fig. 5 Photoluminescence spectra of **2** (a) and **4** (b) in solid state.

As expected, the Zn(II) compound **2** and the Cd(II) compound **4** possess the photoluminescence properties (see Fig. 5). Upon excitation (λ_{ex} = 363 nm for **2**; λ_{ex} = 350 nm for **4**), both emit blue light, and the peaks are centered at 427 nm for **2**, and 430 nm for **4**, respectively. The emissions of both should be assigned to the bcbob-centered electronic excitation ($\pi^* \rightarrow \pi$), since the organic H$_3$(bcbob) molecule exhibits a similar emission (λ_{em} = 425 nm) when excited at 365 nm (see Fig. S10).

(a)   (b)
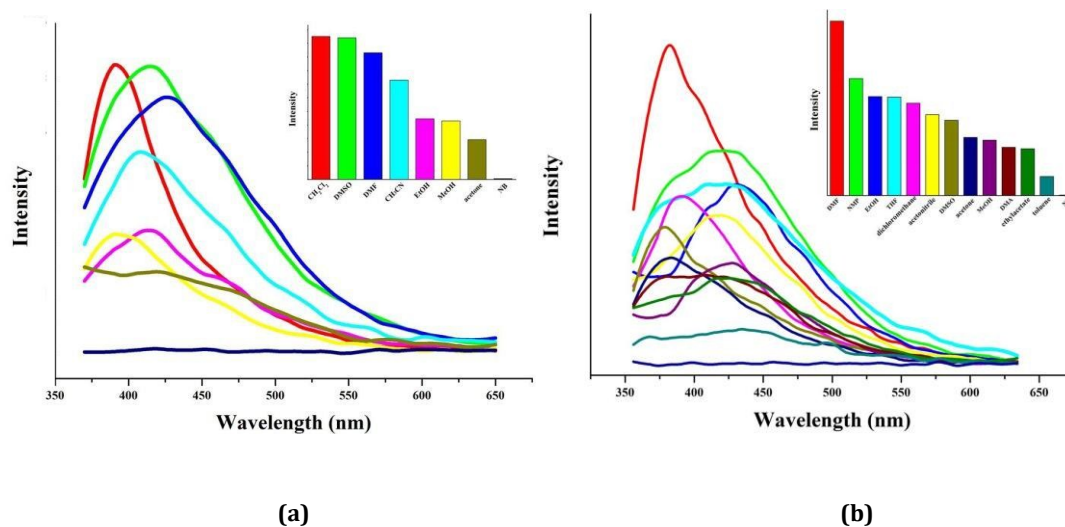
Fig. 6 Photoluminescence behaviors of suspension-state **2** (a) and **4** (b) dispersed in different organic solvents (λ_{ex} = 340 nm for **2**, λ_{ex} = 330 nm for **4**).

In order to reveal the sensing ability of the as-synthesized CP materials, the photoluminescence behaviors of the suspension-state **2** and **4** dispersed in the different organic solvents were investigated. The selected organic solvents have CH$_2$Cl$_2$, DMSO (dimethylsulfoxide), DMF (N,N'-dimethyl formamide), MeOH, EtOH, CH$_3$CN, acetone, DMA (N,N'-dimethylacetamide), NMP (N-methylpyrrolidone), toluene, acetonitrile and NB. Before measurement, a series of stable emulsions were prepared as below: a finely ground powder sample (5 mg) was immersed in an organic solvent (5.00 mL), treated by ultrasonication for 30 min, and then aged for 3 days. As shown in Fig. 6, dispersed in the other organic solvents, the suspensions of compounds **2** and **4** all emits light. It exhibits a similar emission to that of the solid-state sample. Only a minor red- or blue-shift is

observed, which might be associated with the solvated effect.[11] The emission intensities for all of the emulsions exhibit the differences. For compound **2**, CH_2Cl_2, DMF and DMSO are proved to be the strongest enhancers, whereas dispersed in DMF, the suspension of **4** shows the maximum. However, the suspensions of compounds **2** and **4** exhibit a special emission behavior, when dispersed in NB (nitrobenzene). The emissions are completely quenched by NB, which suggests that compounds **2** and **4** can both serve as a sensor to detect the NB molecule. After the measurements, the solid particles are filtered from the suspensions. Fig. S11 gives the XRD patterns of these solid particles. For compound **2**, the experimental XRD patterns are in agreement with the simulated, suggesting that compound **2** is stable in the organic solvents. While for compound **4**, in some organic solvent, it is stable. But in some solvents, **4** is unstable, and the XRD patterns show a little difference.

(a)	**(b)**
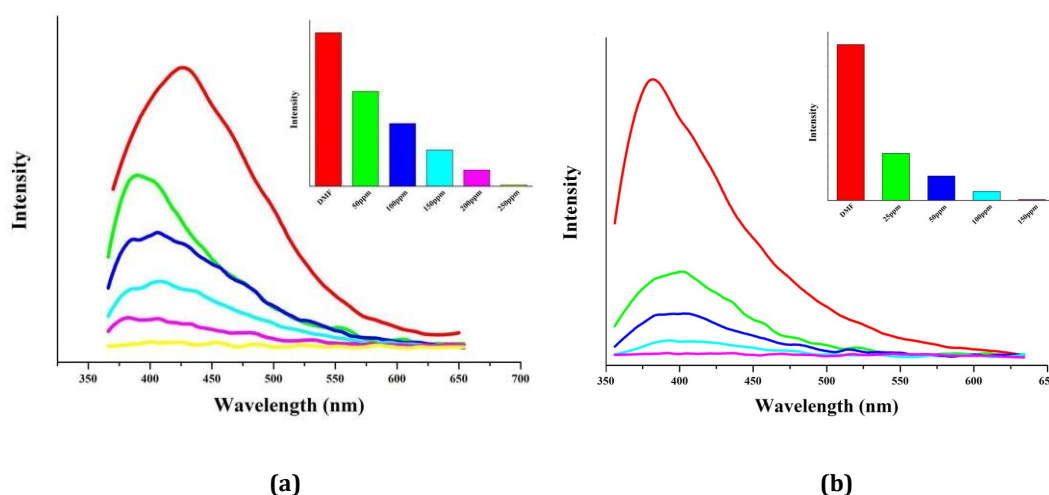
Fig. 7 Photoluminescence behaviors of suspension-state **2** (a) and **4** (b) with gradually increased NB concentrations (dispersible solvent: DMF for both; λ_{ex} = 340 nm for **2**, λ_{ex} = 330 nm for **4**).

In order to investigate the quenching efficiency of the NB molecule, the emission behaviors of the suspensions of **2** and **4** with the gradually increased NB concentrations were measured. DMF is selected to act as the dispersible solvent for both. The selection of the dispersible solvent is based on two rules: (i) dispersed in this solvent, the suspension should have the stronger emission; (ii) dispersed in this solvent, the sample should be stable. As shown in Fig. 7, for both, the emission intensity of the suspensions gradually decrease with the increasing of the NB concentration. When 250 ppm NB is added, the emission of compound **2** is thoroughly quenched, while with the addition of 150 ppm NB, the emission intensity of compound **4** decreases to zero. This implies that compound **2** can sense 250-ppm NB, whereas compound **4** can detect 150-ppm NB. DMSO is also selected to displace DMF to serve as the dispersible solvent of **2**. But dispersed in DMF, compound **2** only detects NB with the concentration of 350 ppm. This suggests that the dispersible solvent affects the quenching efficiency.

In order to investigation the origin of the photoluminescence from the suspensions, the solid particles in the suspensions (**2/4** + dispersible solvent) are removed, and the emission behaviors of the mother solutions are measured. As shown in Fig. S12, even though the mother solutions also possess the photoluminescence emissions, the intensity is by far weaker than that of the suspensions. This implies that the photoluminescence from the suspensions is mainly derived from the as-synthesized CP.

The bcbob molecule is an electron-rich aromatic ligand (potential electron donor), while the NB molecule possesses the electron deficient nature (potential electron acceptor). The good dispersible nature of the

as-synthesized CP particles in the organic solvent makes the introduced NB molecule access easily these particles and be closely adsorbed on the surface of these particles. Due to the close contact, the excited-state electron transfer path of the compound is changed. The excited-state electron would undergo a transfer to the high electron-withdrawing -NO_2 group in the NB molecule, instead of returning to the ground-state energy level. So the quenching is observed. Based on the statements above, maybe these three factors play a key role in determining the sensing ability of the CP material on NB: (i) the size of the solid particle. The smaller particles possess the larger surface area, and are easily dispersed evenly in the organic solvent; (ii) a good dispersible nature of these solid particles in the organic solvent. The larger surface area as well as the better dispersant for the solid particles is helpful to the attachment of the mixed trace NB molecule; (iii) the larger π-conjugated structure of the organic ligand in the CP framework. The molecule with the larger π-conjugated structure will give a quick photoluminescence response, when encountering NB.[12]

Conclusion

In summary, we employed a tripodal tricarboxylic acid, namely H_3(bcbob), to self-assemble four new 3-D coordination polymers with the assistance of various organic base molecules. Note that the bcbob-based coordination polymers were still less investigated. Synthetically, the pH level of the reactive system is confirmed to be the crucial factor in controlling the crystal growth. It directly affects the deprotonation reaction of the H_3(bcbob) molecule. Meanwhile, it controls the existing form of the mixed organic based molecule, a protonated form or a non-protonated form. X-ray single-crystal analysis reveals that the bcbob molecules can generally link the metal centers into a 3-D network. The role of the incorporated organic base molecule is mainly to stabilize the 3-D metal-bcbob network in the diverse ways: (i) acting as a guest molecule; (ii) acting as a pillar, supporting the channel. If the bcboc molecules only link the metal centers into an oligomer, the mixed organic base molecule serves as the second linkers, extending the oligomers into a 3-D network. At this time, the interpenetration maybe occurs, in order to form a 3-D stable network. A series of photoluminescence analyses of compounds **2** and **4** in the suspension state indicate that (i) compounds **2** and **4** can serve as the sensors to detect the ppm-grade NB; (ii) dispersed in the different solvent, the sensing ability for the compound maybe exhibits a little difference; (iii) the photoluminescence quenching maybe derives from three factors: electron-rich nature for the metal-multicarboxylate CP; the electron-withdrawing nature for NB; a well dispersible nature of the metal-multicarboxylate CP particles in the organic solvent; (iv) the additional NB molecule alters the excited-state electron transfer path, resulting in the photoluminescence quenching.

Acknowledgements

References

1 (*a*) H. Zhou and S. Kitagawa, *Chem. Soc. Rev.*, 2014, **43**, 5415-5418; (*b*) M. Eddaoudi, D. F. Eubank, K. Adil and V. Guillerm, *Chem. Soc. Rev.*, 2015, **44**, 228-249; (*c*) C. K. Brozek and M. Dincă, *Chem. Soc. Rev.*, 2014, **43**, 5456-5467; (*d*) Q. Zhu and Q. Xu, *Chem. Soc. Rev.*, 2014, **43**, 5468-5512; (*e*) W. Lu, Z. Wei, Z. Gu, T. Liu, J. Park, J. Park, J. Tian, M. Zhang, Q. Zhang, T. Gentle III, M. Bosch and H. Zhou, *Chem. Soc. Rev.*, 2014, **43**, 5561-5593; (*f*) S. Furukawa, J. Reboul, S. Diring, K. Sunida and S. Kitagawa, *Chem. Soc. Rev.*, 2014, **43**, 5700-5734; (*g*) A. Schneemann, V. Bon, I. Schwedler, I. Senkovska, S. Kaskel and R. A. Fischer, *Chem. Soc. Rev.*, 2014, **43**, 6062-6096; (*h*) D. Prochowicz, K. Sokolowski and J. Lewiński, *Coord. Chem. Rev.*, 2014, **270**, 112-126; (*i*) Y. N. Wang, Q. F. Yang, G. H. Li, P. Zhang, J. H. Yu and J. Q. Xu, *Dalton Trans.*, 2014, **43**,

11646-11657; (*j*) Y. N. Wang, F. Q. Bai, J. H. Yu and J. Q. Xu, *Dalton Trans.*, 2013, **42**, 16547-16555; (*k*) B. Mu, F. Li, Y. Huang and K. S. Walton, *J. Mater. Chem.*, 2012, **22**, 10172-10178; (*l*) T. H. Park, A. J. Hickman, K. Koh, S. Martin, A. G. Wong-Foy, M. S. Sanford and A. J. Matzger, *J. Am. Chem. Soc.*, 2011, **133**, 20138-2041; (*m*) P. Wu, C. He, J. Wang, X. Peng, X. Li, Y. An and C. Duan, *J. Am. Chem. Soc.*, 2012, **134**, 14991-14999; (*n*) L. C. Wang, J. Sun, Z. T. Huang and Q. Y. Zheng, *Cryst. Growth Des.*, 2013, **13**, 1-5; (*o*) P. V. Dau, K. K. Tanabe and S. M. Cohen, *Chem. Commun.*, 2012, **48**, 9370-9372; (*p*) D. Kim, X. Liu and M. S. Lah, *Inorg. Chem. Front.*, 2015, **2**, 336-360; (*q*) B. Tzeng, T. Chang, M. Tsai, Y. Lin, S. Lee and H. Sheu, *ChemPlusChem*, 2015, **80**, 878-885; (*r*) B. Tzeng, C. Yeh and T. Chang, *ChemPlusChem*, 2014, **79**, 387-393.

2 (*a*) A. Dhakshinamoorthy, A. M. Asiri and H. Garcia, *Chem. Soc. Rev.*, 2015, **44**, 1922-1947; (*b*) D. Bradshaw, S. E. Hankari and L. L. Spagnolo, *Chem. Soc. Rev.*, 2014, **43**, 5431-5443; (*c*) A. Dhakshinamoorthy and H. Garcia, *Chem. Soc. Rev.*, 2014, **43**, 5750-5765; (*d*) T. Zhang and W. Lin, *Chem. Soc. Rev.*, 2014, **43**, 5982-5993; (*e*) A. Schwarzer, T. Saplinova and E. Kroke, *Coord. Chem. Rev.*, 2013, **257**, 2032-2062; (*f*) Y. Zhou and B. Yan, *Inorg. Chem.*, 2014, **53**, 3456-3463; (*o*) J. Heine and K. M. Buschbaum, *Chem. Soc. Rev.*, 2013, **42**, 9232-9242; (*g*) Y. N. Wang, J. H. Yu and J. Q. Xu, *Inorg. Chem. Front.*, 2014, **1**, 673-681; (*h*) Y. N. Wang, G. H. Li, F. Q. Bai, J. H. Yu and J. Q. Xu, *Dalton Trans.*, 2014, **43**, 15617-15627; (*i*) Y. Lu and B. Yan, *Chem. Commun.*, 2014, **50**, 15443-15446; (*j*) L. V. Mever, F. Schönfeld and K. M. Buschbaum, *Chem. Commun.*, 2014, **50**, 8093-8108; (*k*) R. F. Mendes and F. A. A. Paz, *Inorg. Chem. Front.*, 2015, **2**, 495-509; (*l*) P. Bose, L. Bai, R. Ganguly, R. Zou and Y. Zhao, *ChemPlusChem*, 2015, **80**, 1259-1266; (*m*) L. Wang, Y. Li, F. Yang, Q. Liu, J. Ma and Y. Dong, *Inorg. Chem.*, 2014, **53**, 9087-9084.

3 (*a*) E. Barea, C. Montoro and J. A. R. Navarro, *Chem. Soc. Rev.*, 2014, **43**, 5419-5430; (*b*) D. Bradshaw, S. El-Hankari and L. Lupica-Spagnolo, *Chem. Soc. Rev.*, 2014, **43**, 5431-5443; (*c*) J. Canivet, A. Fateeva, Y. Guo, B. Coasne and D. Farrusseng, *Chem. Soc. Rev.*, 2014, **43**, 5594-5617; (*d*) B. V. Voorde, B. Bueken, J. Denayer and D. D. Vos, *Chem. Soc. Rev.*, 2014, **43**, 5766-5788; (*e*) X. Wang, J. Luan, H. Lin, Q. Lu, M. Le, G. Liu and J. Shao, *ChemPlusChem*, 2014, **79**, 1691-1702; (*f*) B. Liu, Y. H. Jiang, Z. S. Li, L. Hou and B. Liu, *Inorg. Chem. Front.*, 2015, **2**, 550-557; (*g*) X. L. Qi, J. W. Ye, R. B. Liu, P. Q. Liao, S. Y. Liu, C. T. He, J. P. Zhang and X. M. Chen, *Inorg. Chem. Front.*, 2015, **2**, 136-140; (*h*) X. Duan, J. Yu, J. Cai, Y. He, C. Wu, W. Zhou, T. Yildirim, Z. Zhang, S. Xiang, M. O'Keeffe, B. Chen and G. Qian, *Chem. Commun.*, 2013, **49**, 2043-2045; (*i*) Y. Xiong, Y. Fan, R. Yang, S. Chen, M. Pan, J. Jiang and C. Su, *Chem. Commun.*, 2014, **50**, 14631-14634; (*j*) Z. Zhu, Y. Bai, L. Zhang, D. Sun, J. Fang and S. Zhu, *Chem. Commun.*, 2014, **50**, 14674-14677; (*k*) Z. Niu, S. Fang, J. Ma, X. Zhang and P. Cheng, *Chem. Commun.*, 2014, **50**, 7797-7799; (*l*) R. Wang, Q. Meng, L. Zhang, H. Wang, F. Dai, W. Guo, L. Zhao and D. Sun, *Chem. Commun.*, 2014, **50**, 4911-4914; (*m*) Q. Yan, Y. Lin, C. Kong and L. Chen, *Chem. Commun.*, 2013, **49**, 6873-6875; (*n*) Z. Zhang, Y. Zhao, Q. Gong, Z. Li and J. Li, *Chem. Commun.*, 2013, **49**, 653-661; (*o*) C. H. Lee, J. Y. Wu, G. H. Lee, S. M. Peng, J. C. Jiang and K. L. Lu, *Inorg. Chem. Front.*, 2015, **2**, 477-484.

4 (*a*) Z. Hu, B. J. Deibert and J. Li, *Chem. Soc. Rev.*, 2014, **43**, 5815-5840; (*b*) Y. Cui, B. Chen and G. Qian, *Coord. Chem. Rev.*, 2014, **273**, 76-86; (*c*) X. Zhang, W. Wang, Z. Hu, G. Wang and K. Uvdal, *Coord. Chem. Rev.*, 2015, **284**, 206-235; (*d*) L. Qin, M. Zheng, Z. Guo, H. Zheng and Y. Xu, *Chem. Commun.*, 2015, **51**, 2447-2449; (*e*) W. Shi, A. Cui and H. Kou, *ChemPlusChem*, 2014, **79**, 310-317; (*f*) J. Hao and B. Yan, *J. Mater. Chem. A*, 2014, **2**, 18018-18025; (*g*) Y. Li, L. Wang, B. Zhou, Q. Chen and X. Bu, *J. Mater. Chem. A*, 2013, **1**, 495-499; (*h*) Z. Xiang, C. Fang, S. Leng and D. Cao, *J. Mater. Chem. A*, 2014, **2**, 7662-7665; (*i*) L. Liu, X. Chen, J. Qiu and C. Hao, *Dalton Trans.*, 2015, **44**, 2897-2906; (*j*) S. Pramanik, Z. Hu, X. Zhang, C. Zheng, S. Kelly and J. Li, *Chem. Eur. J.*, 2013, **19**, 15964-15971; (*k*) D. Banerjee, Z. Hu and J. Li, *Dalton Trans.*, 2014, **43**, 10668-10685; (*l*) Z. Hu, B. J. Deibert and J. Li, *Chem. Soc. Rev.*, 2014, **43**, 5815-5840; (*l*) Y. Rachuri, B. Parmar, K. K. Bisht and E. Suresh, *Inorg. Chem. Front.*, 2015, **2**, 228-236; (*m*) X. Q. Zhao, P. Cui, B. Zhao, W. Shi and P. Cheng, *Dalton Trans.*, 2011, **40**, 805-819; (*o*) Y. L. Hou, H. Xu, R. R. Cheng and B. Zhao, *Chem. Commun.*, 2015, **51**, 6769-6772.

5 (*a*) E. Coronado and G. M. Espallarqas, *Chem. Soc. Rev.*, 2013, 42, 1525-1539; (*b*) L. Cao, Y. Wei, C. Ji, M. Ma, S. Zang and T. C. W. Mark, *Chem. Asian J.*, 2014, **9**, 3094-3098; (*c*) D. Shao, S. Zhang, X. Zhao and X. Wang, *Chem. Commun.*, 2015, **51**, 4360-4363; (*d*) S. I. Vasylevs'kyy, G. A. Senchyk, A. B. Lysenko, E. B. Rusanov, A. N. Chernega, J. Jezierska, H. Krautscheid, K. V. Domasevitch and A. Ozarowski, *Inorg. Chem.*, 2014, **53**, 3642-3654; (*e*) P. Manna, B. K. Tripuramallu, S.Bommakanti and S. K. Das, *Dalton Trans.*, 2015, **44**, 2852-2864; (*f*) S. Adhikari, A. Banerjee, S. Nandi, M. Fondo, J. Sanmartín-Matalobos and D. Das, *Rsc Adv.*, 2015, **5**, 10987-10993; (*g*) S. S. P. Dias, M. V. Kirillova, V. André, J, Ktak and A. M. Kirillov, *Inorg. Chem. Front.*, 2015, **2**, 525-537; (*i*) J. Xie, H. Shu, H. Hu, Z. Han, S. Shen, F. Yuan, M. Yang, F. Dong and G. Xue, *ChemPlusChem*, 2014, **79**, 985-994.

6 S. S. -Y. Chui, S. M.-F. Lo, J. P. H. Charmant, A. G. Orpen and I. D. Williams, *Sciences*, 1999, **283**, 1148-1150.

7 (*a*) S. Chen, Q. Zhai, S. Li, Y. Jiang and M. Hu, *Inorg. Chem.*, 2015, **54**, 10-12; (*b*) B. Dong, L. Chen, S. Zhang, J. Ge, L. Song, H. Tian, Y. Teng and W. Liu, *Dalton Trans.*, 2015, **44**, 1435-1440; (*c*) C. Zhan, S. Ou, C. Zou, M. Zhao and C. Wu, *Anal. Chem.*, 2014, **86**, 6648-6653; (*d*) C. Zhan, C. Zou, G. Kong and C. Wu, *Cryst. Growth Des.*, 2013, **13**, 1429-1437; (*e*) A. Bajpai, P. Chandrasekhar, S. Govardhan, R. Banerjee and J. N. Moorthy, *Chem. Eur. J.*, 2015, **21**, 2759-2765; (*f*) K. Peikert, F. Hoffmann and M. Fröba, *CrystEngComm*, 2015, **17**, 353-360; (*g*) P. Du, Y. Yang, Y. Liu, W. Kan and J. Ma, *CrystEngComm*, 2013, **15**, 6986-7002; (*h*) L. Chen, L. Zhang, S. Li, Y. Qiu, K. Shao, X. Wang and Z. Su, *CrystEngComm*, 2013, **15**, 8214-8221; (*i*) H. Fu, F. Wang and J. Zhang, *Dalton Trans.*, 2014, 43, 4668-4673; (*j*) P. Wu, C. He, J. Wang, X. Peng, X. Li, Y. An and C. Duan, *J. Am. Chem. Soc.*, 2012, **134**, 14991-14999; (*k*) W. H. Huang, X. J. Luan, X. Zhou, J. Chen and Y. Y. Wang, *CrystEngComm*, 2013, **15**, 10389-10398; (*l*) Q. Tang, S. Liu, Y. Liu, D. He, J. Miao, X. Wang, Y. Ji and Z. Zheng, *Inorg. Chem.*, 2014, **53**, 289-293; (*m*) J. Cui, Y. Li, Z. Guo and H. Zheng, *Chem. Commun.*, 2013, **49**, 555-557; (*n*) K. Peikert, F. Hoffmann and M. Fröba, *Chem. Commun.*, 2012, **48**, 11196-11198; (*o*) C. Janiak, *Chem. Commun.*, 2013, **49**, 6933-6937; (*p*) Y. P. He, Y. X. Tan and J. Zhang, *Inorg. Chem.*, 2012, **51**, 11232-11234; (*q*) J. Park, J. R. Li, E. C. Sañudo, D. Yuan and H. C. Zhou, *Chem. Commun.*, 2012, **48**, 883-885; (*r*) W. H. Huang, G. P. Yang, J. Chen, X. Chen. C. P. Zhang, Y. Y. Wang and Q. Z. Shi, *Cryst. Growth Des.*, 2013, **13**, 66-73; (*s*) H. Furukawa, M. A. Miller and O. M. Yaghi, *J. Mater. Chem.*, 2007, **17**, 3197-3204; (*t*) Y. P. He, Y. X. Tan and J. Zhang; *Inorg. Chem.*, 2013, **52**, 12758-12762; (*u*) F. Gándara, H. Furukawa, S. Lee and O. M. Yaghi, *J. Am. Chem. Soc.*, 2014, **136**, 5271-5274; (*v*) H. Furukawa, Y. B. Go, N. Ko, Y. Y. Park, F. J. Uribe-Romo, J. Kim, M. O'Keeffe and O. M. Yaghi, *Inorg. Chem.*, 2011, **50**, 9147-9152.

8 (*a*) R. Patra, H. M. Titi and I. Goldberg, *New J. Chem.*, 2013, **37**, 1494-1500; (*b*) X. Zhang, L. Fang, W. Song, W. Fan, L. Sun and X. Zhao, *RSC Adv.*, 2014, **4**, 30274-30281.

9 G. M. Sheldrick, *Acta Crystallogr., Sect. A: Found. Crystallogr.*, 2008, **64**, 112-122.

10 (*a*) J. Meng, Y. Gong, Q. Lin, M. Zhang, P. Zhang, H. Shi and J. Lin, *Dalton Trans.*, 2015, **44**, 5407-5416; (*b*) L. Zhang, T. Song, J. Xu, S. Zeng, Y. Wu, Y. Fan and L. Wang, *CrystEngComm*, 2014, **16**, 2440-2451; (*c*) I. Spanopoulos, P. Xydias, C. D. Malliakas and P. N. Trikalitis, *Inorg. Chem.*, 2013, **52**, 855-862; (*d*) Q. Zheng, F. Yang, M. Deng, Y. Ling, X. Liu, Z. Chen, Y. Wang, L. Weng and Y. Zhou, *Inorg. Chem.*, 2013, **52**, 10368-10374; (*e*) Y. Gai, F. Jiang, L. Chen, Y. Bu, K. Su, S. A. Al-Thabaiti and M. Hong, *Inorg. Chem.*, 2013, **52**, 7658-7665; (*f*) F. Yi, S. Dang, W. Yang and Z. Sun, *CrystEngComm*, 2013, **15**, 8320-8329; (*g*) J. J. Henkelis, S. A. Barnett, L. P. Harding and M. J. Hardie, *Inorg. Chem.*, 2012, **51**, 10657-10674; (*h*) Y. Hu, H. Ma, B. Zheng, W. Zhang, S. Xiang, L. Zhai, L. Wang, B. Chen, X. Ren and J. Bai, *Inorg. Chem.*, 2012, **51**, 7066-7074; (*i*) D. J. Mihalcik, T. Zhang, L. Ma and W. Lin, *Inorg. Chem.*, 2012, **51**, 2503-2508; (*j*) X. Li, F. Jiang, M. Wu, L. Chen, J. Qian, K. Zhou, D. Yuan and M. Hong, *Inorg. Chem.*, 2014, **53**, 1032-1038; (*k*) Y. Gai, F. Jiang, L. Chen, M. Wu, K. Su, J. Pan, X. Wan and M. Hong, *Cryst. Growth Des.*, 2014, **14**, 1010-1017; (*l*)Y. Wei, R. Lin, P. Wang, P. Liao, C. He, W. Xue, L. Hou, W. Zhang, J. Zhang and X. Chen, *CrystEngComm*, 2014, **16**, 6325-6330; (*m*) E. Yang, Y. Zhang,

Z. Liu and X. Zhao, *Inorg. Chem.*, 2014, **53**, 327-335; (*n*) Z. Lin, Y. Huang, T. Liu, X. Li and R. Cao, *Inorg. Chem.*, 2013, **52**, 3127-3132; (*o*) A. Santra, I. Senkovska, S. Kaskel and P. K. Bharadwaj, *Inorg. Chem.*, 2013, **52**, 7358-7366.

11 (*a*) J. Jin, F. Q. Bai, M. J. Jia, Y. N. Wang, H. L. Jia, J. H. Yu and J. Q. Xu, *Dalton Trans.*, 2013, **42**, 8771-8780; (*b*) J. Jin, F. Q. Bai, M. J. Jia, J. H. Yu and J. Q. Xu, *CrystEngComm*, 2013, **15**, 5919-5927.

12 (*a*) Y. N. Wang, P. Zhang, J. H. Yu and J. Q. Xu, *Dalton Trans.*, 2015, **44**, 1655-1663; (*b*) L. Zhou, J. Zhang, Y. Z. Li and H. B. Du, *CrystEngComm*, 2013, **15**, 8989-8997; (*c*) M. Guo and Z. M. Sun, *J. Mater. Chem.*, 2012, **22**, 15939-15946; (*d*) H. Zhang, W. Jiang, J. Yang, Y. Y. Liu, S. Song and J. F. Ma, *CrystEngComm*, 2014, **16**, 9939-9946; (*e*) Y. C. He, H. M. Zhang, Y. Y. Liu, Q. Y. Zhai, Q. T. Shen, S. Y. Song and J. F. Ma, *Cryst. Growth Des.*, 2014, **14**, 3174-3178; (*f*) G. Y. Wang, L. L. Yang, Y. Li, H. Song, W. J. Ruan, Z. Chang and X. H. Bu, *Dalton Trans.*, 2013, **42**, 12865-12868; (*g*) H. Wang, W. Yang and Z. M. Sun, *Chem. Asian. J.*, 2013, **8**, 982-989; (*h*) D. Tian, Y. Li, R. Y. Chen, Z. Chang, G. Y. Wang and X. H. Bu, *J. Mater. Chem. A*, 2014, **2**, 1465-1470; (*i*) B. Gole, A. K. Bar and P. S. Mukherjee, *Chem. Eur. J.*, 2014, **20**, 2276-2291; (*j*) H. Xu, F. Liu, Y. Cui, B. Chem and G. Qian, *Chem. Commun.*, 2011, **47**, 3153-3155; (*k*) S. R. Zhang, D. Y. Du, J. S. Qin, S. L. Li, W. W. He, Y. Q. Lan and Z. M. Su, *Inorg. Chem.*, 2014, **53**, 8105-8113; (*l*) Y. N. Wang, J. H. Yu and J. Q. Xu, *ChemPlusChem.*, 2015, **80**, 1732-1740.